High internal phase emulsion hierarchical porous polymer grafting polyol compounds for boron removal

Zhe Wang[1], Kaiyuan Ma[1], Yufeng Zhang[1], Xinbo Zhang[1*], Huu Hao NGO[1,2*], Jianqiang Meng[3], Lingzhong Du[4]

[1] *Joint Research Center for Protective Infrastructure Technology and Environmental Green Bioprocess, School of Environmental and Municipal Engineering, Tianjin Chengjian University, Tianjin 300384, PR China*

[2] *Centre for Technology in Water and Wastewater, School of Civil and Environmental Engineering, University of Technology Sydney, Sydney, NSW 2007, Australia*

[3] *State Key Laboratory of Separation Membranes and Membrane Processes, Tianjin Polytechnic University, Tianjin 300387, PR China*

[4] *Stat Key Laboratory of Multi-Phase Complex Systems, Institute of Process Engineering, Chinese Academy of Science, Beijing 100190, PR China*

*Corresponding authors: Xinbo Zhang (email:zxbcj2006@126.com); Huu Hao Ngo (email: ngohuuhao121@gmail.com)

Abstract

Removing micro-pollutants is an important global challenge for the development of good adsorbents and environmental engineering issues. In this work, the structure of hierarchically and interconnected porous polymer has been fabricated by a high internal phase emulsion (HIPE) with water-in-oil and used for removing boron from water. This porous polymer was synthesized via monomer radical polymerization and utilized the active sites of monomer –Cl. In this way the vicinal hydroxyl group of N-Methyl-D-glucamine (NMG) was successfully introduced and grafted into HIPE by nucleophilic substitution reaction under the catalysis of triethylamine. The maximum boron uptake capacity was 2.54 mmol/g at a boron concentration of 100 mg/L, and reached adsorption equilibrium after about 2 h. Compared to traditional adsorption membrane materials, the HIPE porous polymer had better mechanical strength and able to resist acid and alkaline in the long-term. Meanwhile the regeneration efficiency of the HIPE30%-g-PNMG porous polymer remained at 100% after being used for 10 cycles.

Keywords: HIPE porous polymer; polymerization; Grafting; Boron removal; Adsorption

1. Introduction

Boron as a micro-nutrient is essential for humans, animals and plants. It is formed from boric acid and borate salts that are commonly found in the hydrosphere and lithosphere [1]. When living organisms take up a small amount of boron, it benefits health and improves carbohydrate metabolism, sugar transport, cell growth, and grain formation [2-4]. However, excessive intake of boron is harmful to an organism. For people, ingesting high concentrations of boron can cause damage to the central nervous and reproductive systems. For plants, excess boron intake will lead to a decline in fruit yield, leaf damage, and adverse effects on root growth. For this reason the World Health Organization (WHO) stipulated boron concentration in drinking water must be limited to 2.4 mg/L while irrigation water is recommended to be in the 0.3 and 1 mg/L range [5]. However, in some water sources, the boron concentration is detected to be well above

the WHO regulation, such as seawater at around 5 mg/L, groundwater in certain areas as high as 100 mg/L, and even some manufacturing industrial wastewater can be more than 1000 mg/L. For this reason, seeking an efficient boron removal treatment technology is very important.

There are many technologies for boron removal currently operating including reverse osmosis (RO) [6], ion exchange, chemical sedimentation, extraction, electrodialysis, flocculation, adsorption, etc. [7-13]. However, these methods of removing boron still need to be refined due to boron having strict pH reaction conditions and high diffusion rate. For removing boron via RO technology, it is usually difficult to completely removal this substance in a single pass RO due to the boron nonionic boric acid existing in the form of natural pH and hydrogen bonding diffusion [6, 14].

The adsorption process is highly efficient in its removal, simple operation, remarkable regeneration performance, etc., so it is deemed to be one of the most effective technologies to removal boron. Selecting the appropriate adsorbents may help this process be very succesful. Chelation reaction is a more effective method for removing boron as it has been employed for the construction of complexing ligand of adjacent hydroxyl groups. These function to chelate with boric acid and thereby achieve the objective of adsorption. Traditional adsorption resin has a granular porous structure. The diffusion adsorption process can be divided into two stages: internal diffusion and external diffusion. Generally, the main influential factor of the adsorption rate is the internal diffusion process, which is due to the mass transfer. Thus, how to improve specific surface area, increase adsorption sites and enhance the adsorption rate is a challenge in industrial applications.

Membrane technology is widely used in water treatment and desalination. The boric acid molecule is an uncharged protonic acid retaining a strong affinity, so it can form hydrogen bonds with the membrane. It can diffuse easily through the membrane because boric acid has a small molecular size and nonionic nature. Meanwhile, the pH of boron solution influences the membrane treatment process to removal boron efficiently, this being due to the boric acid

dissociation and existence in the form of a solution at different pH ranges. In our previous analyses [15-17], we synthesized a series of adsorption membranes such as complexing membrane and mixed matrix membrane for boron removal. The outcome was excellent boron adsorption capacity. However, in the process of regeneration, repeated adsorption and desorption in acid-alkali solution for a long period of time leads to: firstly, a decline in the mechanical properties; secondly, destruction of the microstructure of the membrane; and thirdly, membrane properties not able to remove boron.

HIPE is an effective way to obtain the hierarchical porous polymer foam through radical polymerization with water-in-oil [18-20]. The internal phase of HIPE has a total volume fraction amounting to more than 74%, and the external phase is formed through the polymerization of monomers. The spherical voids' structures are able to increase transport efficiency. As well, the interconnecting holes of HIPE facilitate the solute of internal phase movement, adsorption and removal. The HIPE porous polymer has a high specific surface area and obtains to structure with various porous characteristics by controlling polymerization conditions. For example, these include locus of initiation, polymerization process mechanism, and the cross-linking level of polymerization. HIPE has been applied in various fields including adsorption, filtration, ion capture, controlled release, etc. [21-25].

In this work, we focused on boron adsorption by employing a matrix of styrene-divinylbenzebe HIPE porous polymer. To obtain a vicinal hydroxyl group HIPE porous polymer using the complex ligand to chelate boric acid, we introduced the p-ethylene benzyl chloride as reaction group of HIPE. It can utilize the many active sites of benzyl chloride to react the nucleophilic substitution with N-Methyl-D-glucamine (NMG). A massive hierarchical porous structure in HIPE is expected to improve the boron convective transport rate. The HIPE porous polymer was also investigated and discussed in detail with reference to adsorption isotherm and kinetics.

2. Materials and methods

2.1. Materials

Styrene (ST) was purchased from Tianjin Fuchen Chemical Reagent Factory, China. Divinyl benzene (DVB) was obtained from Beijing J&K Scientific Ltd., China. The boric acid was purchased from Aladdin Biochemical Technology Co., Ltd. The other key experimental materials included p-Vinylbenzyl chloride (VBC), triethylamine, Span80 [26], $K_2S_2O_8$， $CaCl_2$, NMG, azobisisobutyronitrile (AIBN), Curcumine, oxalic acid, while 95% ethyl alcohol was purchased from Tianjin Kemiou Chemical Reagent Co., Ltd., China. DI water was produced by Millipore Milli-Q Advantage A10 (Billeerica, MA, USA). All chemical reagents chosen were of analytical grade.

2.2. HIPE porous polymer preparation

Firstly, the HIPE was prepared through the process of radical polymerization. The continuous phase volume ratios of ST: DVB: VBC were respectively 8:1:1, 7:1:2, and 6:1:3. The 20 Vol. % Span 80 as the emulgator and 0.192 g AIBN as the initiator were added into the three flasks and stirred vigorously until they were completely dissolved. Meanwhile, we continued to inject N_2 in order to remove the dissolved oxygen for 15 min. Then, 0.0005 g $K_2S_2O_8$ and 0.0024 g $CaCl_2$ were dissolved in 24 mL dispersion phase DI water. Subsequently, the solution was added into a three-necked flask drop-by-drop and stirred gently. Following this, the HIPE porous foam was prepared by mixing the water and oil, then stirred rapidly via magnetic stirring at 1200 rpm/min at room temperature with nitrogen protection. Subsequently, the emulsion was transferred to beginning the polymerization reaction under 70 ºC for 16 h. This polymerization reaction was carried out under conditions of sealing with a balloon after being filled with nitrogen for 15 minutes. The Soxhlet extractor served to purge the HIPE porous polymer in order to remove the residual monomer.

2.3. One-pot Synthesis of the glycopolymer HIPE-g-PNMG

In our previous work [4], the adsorbent material was synthesized via ATRP reaction, in an effort to introduce vicinal hydroxyl groups to the process of boron removal. The ATRP needs

to be rigidly controlled and it has multiple reaction steps. In this research, we introduced the glycopolymer using the simple one-step method which employed the triethylamine as a catalyst to obtain the adsorbent. The major phase of the experiment was adding in sequence the water (15 mL), acetone (15 mL), triethylamine (10 mL), and NMG (0.5 g) into the three-necked flask. The mixture was then stirred continuously for 60 ºC over 16 h. The specimen used a Soxhlet extractor for purging for 2 h with DI water and dried in a freeze dryer. The obtained HIPE was respectively represented as HIPE10%-g-PNMG, HIPE20%-g-PNMG, and HIPE30%-g-PNMG according to the VBC content. The synthesis reaction route of the HIPE porous polymer and complexation mechanism are illustrated in Fig. 1 below.

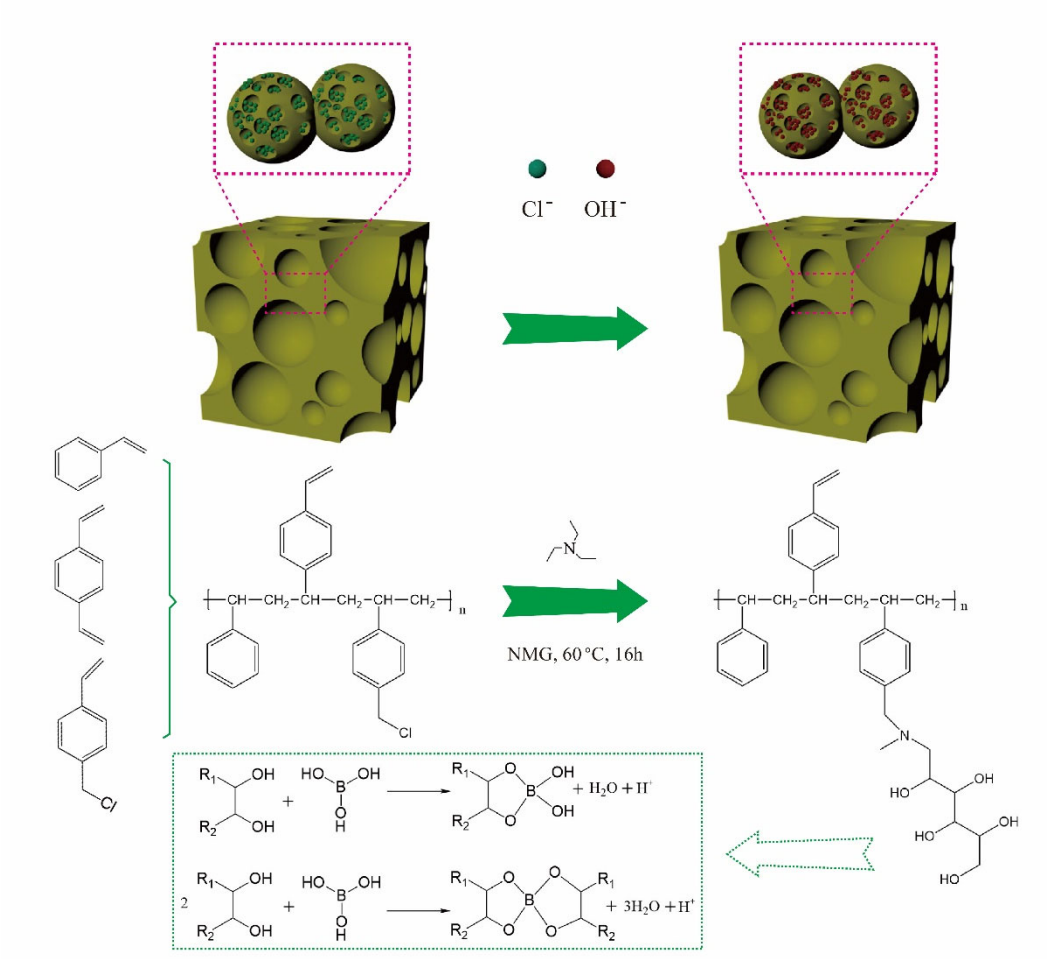

Fig. 1. Diagram of the HIPE porous polymer synthesis and mechanism.

The NMG of HIPE grafting yield value was calculated using the initial and final masses according to the following equation (1):

$$GR = \frac{(W_1 - W_0)}{W_0} \quad (1)$$

where W_1 (mg) and W_0 (mg) were respectively the HIPE-g-PNMG and HIPE weight.

2.4. HIPE porous polymer surface characterization

The Fourier-transform infrared spectrophotometer (FTIR) verified the HIPE porous polymer surface chemical composition (Bruker, Vector-22). X-ray photoelectron spectroscopy (XPS) performed the HIPE (Kratos axis ultra). Surface morphology of the HIPE porous polymer was obtained via scanning electron microscope (SEM, Hitachi S-4800, Japan). The HIPE porous polymer tensile properties according to ISO 1184: 1983 standard were recorded by a SNAS electronic universal testing machine (MTS, China). N_2 adsorption/desorption measurements were performed at 77 K (Quantachrome, ASIQ, USA).

2.5. HIPE porous polymer boron removal experiments

For the static boron adsorption experiment, the HIPE porous polymer specimen was weighed after pre-drying and transferred into a conical flask with high-density polyethylene (HDPE). In this paper, the adsorbent of porous polymer weight was controlled at 0.01 g. This flask contained 50 mL of various concentrations of boric acid solution, and controlled pH in the cell. Then the conical flask was sealed and constantly shaken at 30 ºC for 2 h. The Curcumine method with spectrophotometer served to analyze the boron concentration at the wavelength λ=540 nm [27]. Research into the kinetic adsorption was done by predetermined time intervals to withdraw the boron solution at various boron concentrations. The boron uptake capacity (q) was calculated according to equation (2) below:

$$q = \frac{(c_0 - c_e)V}{mM} \quad (2)$$

where c_0 (mg/L) is the initial boron concentration, c_e (mg/L) is the equilibrium boron concentration, V (L) is the volume solution, m (g) is the weight of dry HIPE or HIPE-g-NMG porous polymer, and M is the boron acid mole weight (g/mol).

2.6. Regeneration of the porous polymer

The acid leaching method helped to research the regenerability of the HIPE porous polymer. The saturated HIPE was soaked and stirred into the HCl solution with 0.1 mol/L for 0.5 h. Then the porous polymer was flushed by DI water and immediately transferred into the NaOH solution with 0.1 mol/L for 0.5 h. The porous polymer used a large amount of DI water that was subjected to rinsing until neutralized and obtained the regenerated porous polymer HIPE.

The HIPE regeneration efficiency (RE) was calculated according to equation (3):

$$RE = \frac{q_2}{q_1} \times 100\% \quad (3)$$

where the q_1 (mmol/g) is the boron uptake capacity of the first adsorption capacity, and q_2 (mmol/g) is the boron uptake capacity of the cycle used.

3. Results and discussion

3.1. HIPE surface compositions

Fig. 2 depicts the FTIR results for the HIPE porous polymer surface composition with various amounts of VBC. Evident are the characteristic features of the C-Cl stretching vibration peak at 710 cm^{-1}. It was clearly seen that the peak intensity of C-Cl increased significantly when an increase in VBC content in the HIPE also occurred. Meanwhile, it indicated there were more active sites on the -Cl. Compared with unmodified HIPE, the HIPE-g-PNMG spectra at 3400 cm^{-1} is pristine with reference to the -OH groups emission peak stretching vibration, which is attributed to the vicinal hydroxyl groups of the NMG terminal chain. The intensity of the -OH peak rose when the VBC content also increased. In addition, the benzene ring skeletal C=C stretching vibration was revealed at 1460 cm^{-1} and 1420 cm^{-1}. The HIPE polymer C=C stretching vibration's moderate intensity peak was evident at 1640 cm^{-1}. The NMG secondary amine of C-N stretching vibration appeared at 1310 cm^{-1}.

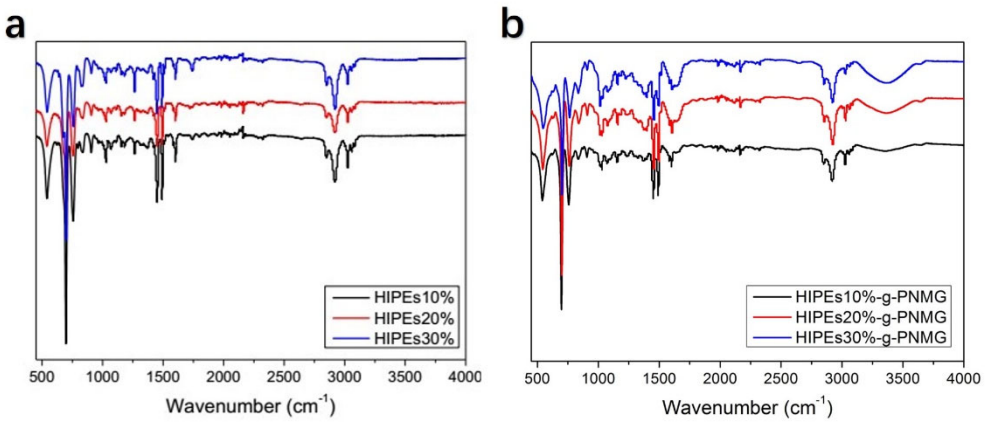

Fig. 2. FTIR spectra of the HIPE (a) and HIPE-g-PNMG (b) with various amounts of VBC.

The HIPE micro-construction was further investigated using XPS. The HIPE unmodified and modified surfaces wide scans and C1s core level spectra are illustrated in Fig. 3. Before HIPE was modified, it revealed the Cl2p emission peaks at 199.8 eV and 285.1 eV emission peaks assigned to C1s (Fig. 3 a and Fig. 3 b). It was observed that the Cl2p peak intensity clearly increased with VBC content. The C1s core level spectra confirmed that the -Cl content further increased at 286.7 eV (Fig. 3 a' and Fig. 3 b'). The modified HIPE porous polymer emission peaks appeared at 197.2 eV, 400.9 eV, and 532.1 eV at the wide spectra, which was attributed to Cl2p, N1s and O1s, respectively (Fig. 3 c and Fig. 3 d). The new spectra indicated that the NMG group was successfully grafted into the HIPE. In addition, the pristine HIPE-g-PNMG C1s emission peaks at 285.4 eV and 287.2 eV were attributed to C-O and C-N spectra. When comparing Fig. 3 a' and Fig. 3 b', the spectrum intensity of C-Cl obviously decreased, and the spectra of C-N and C-O then emerged. This was explained by the glycopolymer being introduced into the HIPE instead of the chloride group via the reaction process.

It is worth noting here that the spectra intensity of C-N and C-O in Fig. 3 d' was stronger than in the spectrum shown in Fig. 3 c'. It was due to HIPE30%-g-PNMG having more -Cl from VBC group and this made it possible to obtain vicinal hydroxyl groups with secondary amine derived from the NMG reaction. The corresponding HIPE porous polymer element composition is shown in Table 1. We can clearly see that the oxygen element content and ratio of O/Cl dramatically increased. What was also verified was that many vicinal hydroxyl groups

were introduced into the HIPE porous polymer. These results demonstrated that we successfully grafted the NMG and introduced the glycopolymer into the HIPE porous polymer.

Table 1

The HIPE and HIPE-g-PNMG porous polymer elemental surface compositions.

polyHIPE	Atomic percent (mol%)				Atomic ratio
	C	N	Cl	O	O/Cl
HIPE10%	97.48	0	2.52	0	0
HIPE30%	84.59	0	15.41	0	0
HIPE10%-g-PNMG	88.46	1.97	0.9	8.67	9.63
HIPE30%-g-PNMG	83.23	2.19	0.32	14.26	44.56

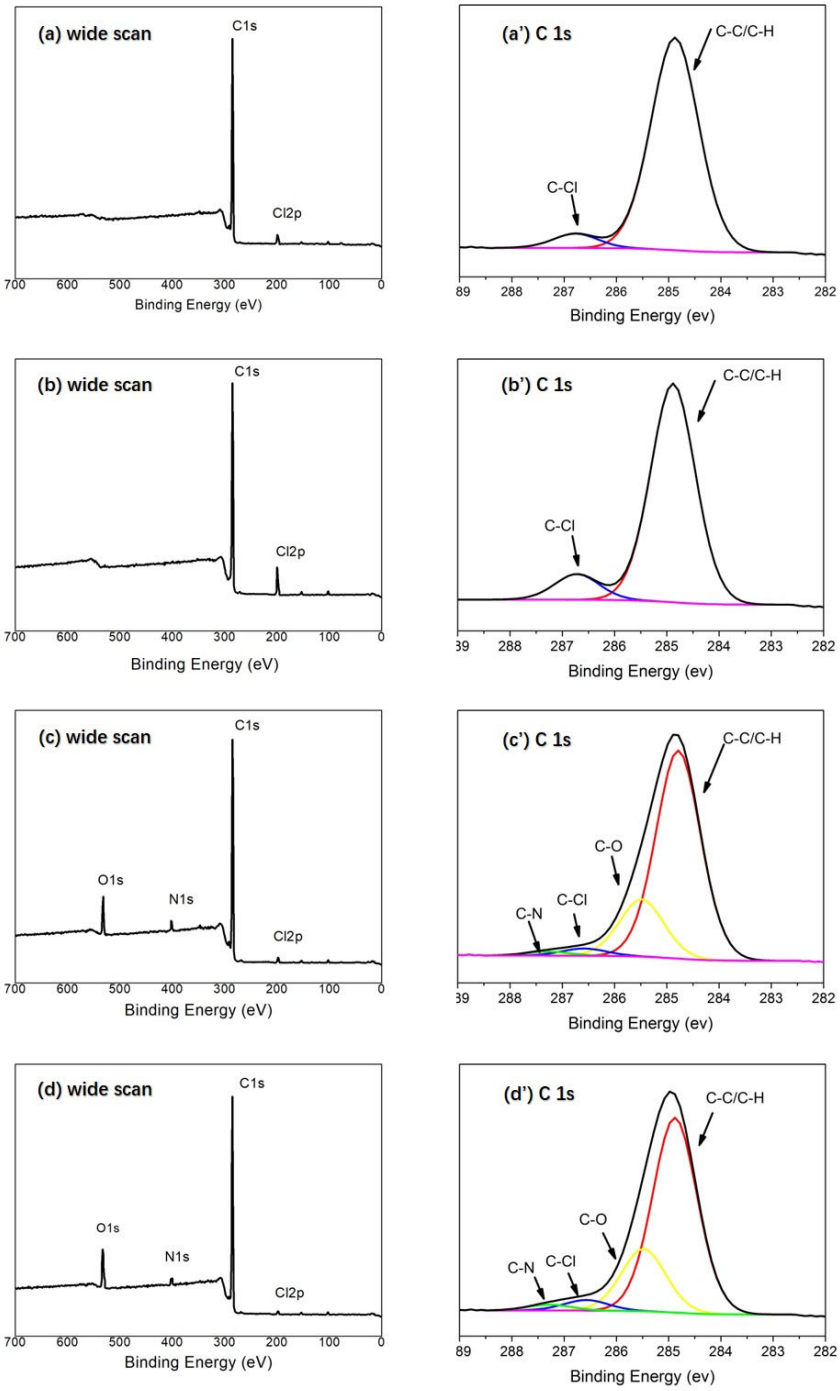

Fig. 3. XPS wide spectra and C1s core level spectra of HIPE (a, a'), HIPE30% (b, b'), HIPE10%-g-PNMG (c, c') and HIPE30%-g-PNMG (d, d').

3. 2. Surface morphology of HIPE

Fig. 4 shows the HIPE porous polymer exhibiting a clearly visible interconnected porous structure. The windows of HIPE were formed via continuous phase polymerization reaction, and the voids were produced by the droplets triggered by dispersion phase evaporation. It

emerged that when the VBC content of HIPE amounted to 10%, the voids of the porous polymer were small and HIPE had a distinct hole of the wall. With the increase in VBC content, the voids' structure visible appeared to be an anomaly, which is especially the case for the VBC content at 30%. It clearly indicated that the voids' diameter increased significantly as shown in the Ostwald ripening process [28-30]. After the NMG was grafted onto the HIPE, the SEM revealed a thin skin polymer layer on the surface of the porous HIPE. However, the microstructure of HIPE-g-PNMG and especially the void indicated no apparent visible change. This outcome confirmed that the void sizes were tunable by altering the VBC content.

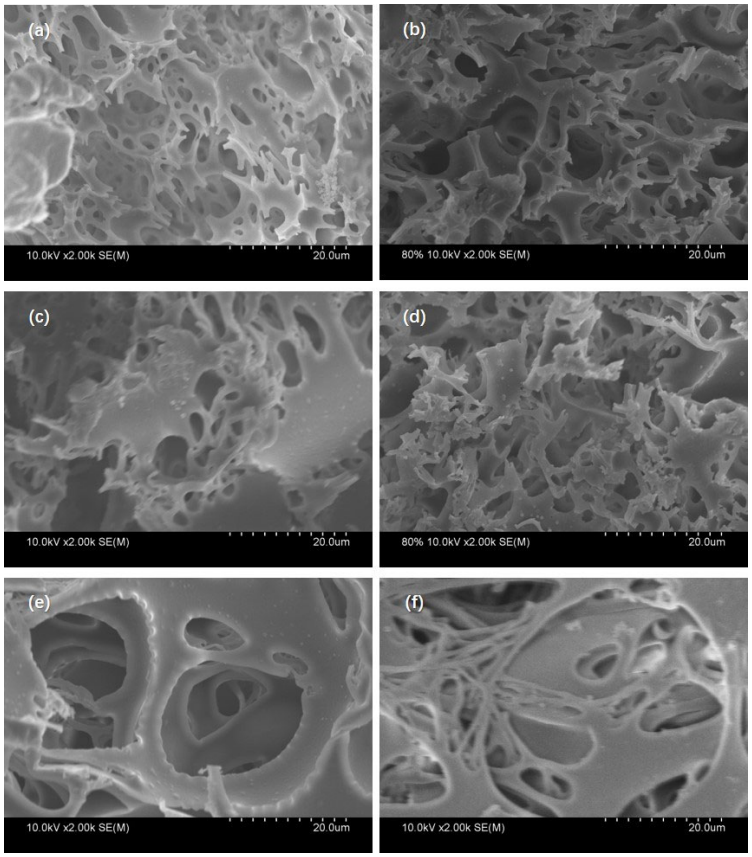

Fig. 4. FESEM images of porous polymer (×2000): (a) HIPE10%, (b) HIPE10%-g-PNMG, (c) HIPE20%, (d) HIPE20%-g-PNMG, (e) HIPE30%, (f) HIPE30%-g-PNMG.

3. 3. Grafting density and physical property of HIPE-g-PNMG

Fig. 5a reveals the increase of VBC content led to the grafting yield ratio gradually increasing, and this was due to the increase in the group of –Cl making the introduction of vicinal hydroxyl groups possible. Establishing the HIPE-g-PNMG mechanical strength was done through the

tension test and results are shown in Fig. 5b. It was discovered that the VBC content increased when the ST content also rose. It presented the pore crush that was due to the decline in mechanical strength of the HIPE porous polymer, which led to brittle fractures occurring easily. This is explained by the ST content decline leading to a fall in the molecular weight of the HIPE porous polymer and reduced the crystal molecular chain entanglement [31, 32]. In addition, the HIPE porous polymer specific surface area was determined by N_2 adsorption/desorption isotherms measurement and the result was shown in Fig.5c. The results indicated that the HIPE30%-g-PNMG has an open-cell structure with BET surface area of 21.92 m^2/g. The visible hysteresis loop was conforming to a type IV isotherms [33]. Pore size distribution of HIPE30%-g-PNMG was calculated using the BJH method. The results revealed the HIPE-g-PNMG has a complex porous structure mainly including mesopores and macropores [34]. During the experiment we tried to add more VBC to improve the grafting rate and introduced vicinal hydroxyl groups, but the mechanical strength and pore size observed from SEM of HIPE-g-PNMG fell persistently. Therefore, the amount of VBC added in the HIPE was controlled within 30% to balance the mechanical strength and quantity of HIPE active sites.

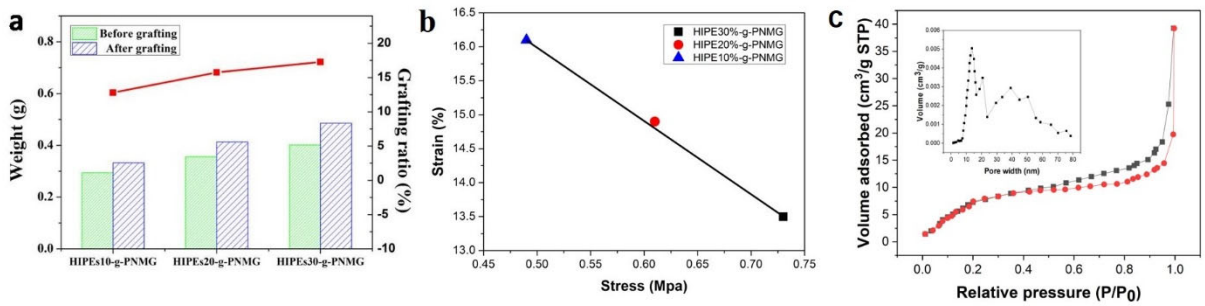

Fig. 5. HIPE-g-PNMG porous polymer grafting ratio (a), mechanical properties (b) and N_2 adsorption/desorption isotherms and pore size distributions of HIPE-g-PNMG.

3.4. Initial boron concentration effect and adsorption isotherm

The standard curve was used to investigate accurately the boron adsorption performance. It obtained the regression equation Y=3.200X-0.080, and the linearly dependent coefficient R^2 was 0.999. Fig. 6a shows the HIPE30%-g-PNMG boron uptake capacity with the influence wielded by the initial boron concentration. The initial concentrations of boron solution prepared

were 4.97 mg/L, 18.33 mg/L, 48.60 mg/L, 99.72 mg/L, 194.79 mg/L and 277.36 mg/L, respectively. These suggested that the initial boron concentration increase led to the boron sorption capacity also increasing. The maximum boron adsorption capacity was recorded as being 2.54 mmol/g, and revealed adsorption plateau when the boron concentration of the solution was more than 100 mg/L. It is worth noting that boron adsorption capacity was calculated via the whole HIPE hierarchical porous polymer rather than the grafting layer. During the process of adsorption, the interconnected porous structures of HIPE helped to form a percolating network, and increased the adsorption capacity via the active sites of grafted the vicinal hydroxyl groups. The HIPE porous polymer's adsorption isotherm was investigated to analyze the boron adsorption mechanism. Fig. 6 b depicts the adsorption isotherms of the HIPE30%-g-PNMG porous polymer. Experimental results were analyzed by utilizing the three models including Langmuir, Freundlich and Dubinin-Radushkevich. The Langmuir followed equation (4) as written here:

$$q_{eq} = \frac{q_{max} b c_{eq}}{1 + b c_{eq}} \quad (4)$$

where q_{eq} is the adsorption equilibrium capacity (mmol/g), c_{eq} is the equilibrium concentration (mg/L), q_{max} is the maximum boron adsorption capacity of saturation (mmol/g), and b is the sorption coefficient (L/mg).

The Freundlich model was obtained using equation (5):

$$q_{eq} = K_f c_{eq}^{1/n} \quad (5)$$

where K_f is a constant (mmol/g), and 1/n represents the intensity constant.

The Dubinin-Radushkevich model has the form of equation (6):

$$q_{eq} = X_m e^{-(k\varepsilon^2)} \quad (6)$$

where ε is Polanyi potential, according to the equal to $RT\ln(1+1/c_{eq})$, the c_{eq} is the equilibrium boron concentration (mol/L), X_m is the adsorption capacity (mmol/g), k is the adsorption energy constant (mol^2/kJ^2), T is the temperature (K, in this paper, the ambient temperature is 298.15 K), and R is the gas constant (kJ • K/mol).

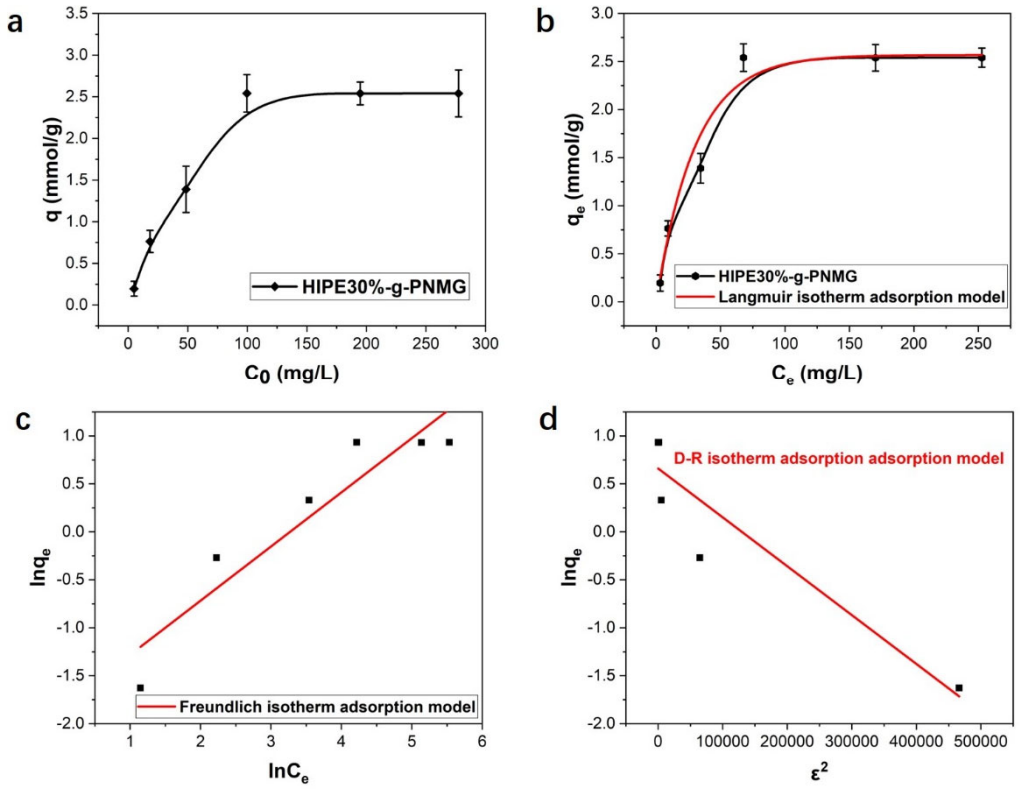

Fig. 6. Effects of initial boron concentration for the HIPE30%-g-PNMG adsorption capacity (a), and adsorption isotherm model of Langmuir (b), Freundlich(c), and D-R (d) fitted curve

Table 2 below shows the fitted curve results and isotherm correlation parameters. We found that the Langmuir isotherm adsorption model was better at describing the HIPE30%-g-PNMG sorption isotherm process. It indicated that the surface of the porous polymer had a homogeneous monolayer which demonstrated two things: firstly, the constant adsorption energy; and secondly, the adsorption process occurred as a reaction of chemical complexation between the adsorption sites of the vicinal hydroxyl group onto the HIPE and boric acid.

Table 2

List of isotherm parameters for boron adsorption.

Porous polymer	Langmuir constants			Freundlich constants			D-R constants		
	q_{max} (mmol/g)	b (L/mg)	R^2	K_f (mmol/g)	1/n	R^2	Xm (mmol/g)	k (mol^2/kJ^2)	R^2
HIPEs30%-g-PNMG	2.57	0.03	0.98	0.16	0.56	0.88	1.94	$0.05*10^{-4}$	0.83

3.5. Adsorption kinetics

The HIPE30%-g-PNMG porous polymer adsorption kinetic was investigated at three boric acid solution concentrations of 5 mg/L, 50 mg/L, and 100 mg/L. Fig. 7a shows the results of adsorption kinetics. It means that the boron adsorption significantly increased as time passed during the incipient stage. Subsequently, the adsorption equilibrium plateau appeared at about 120 min. The kinetic equation of Lagergren pseudo-first-order (PFO) (7), pseudo-second-order (PSO) (8) and intraparticle diffusion (9) were analyzed so that the process of kinetic sorption could be understood.

PFO model equation (7):

$$q_t = q_e(1 - \frac{1}{e^{k_1 t}}) \quad (7)$$

PSO model equation (8):

$$q_t = \frac{k_2 q_e^2 t}{1 + k_2 q_e t} \quad (8)$$

Intraparticle diffusion model equation (9):

$$q_t = k_p t^{1/2} \quad (9)$$

where q_t is the t time boron intake, q_e is the adsorption equilibrium capacity, k_1, k_2 and k_p are respectively the rate constant for PFO, PSO and intraparticle diffusion (min^{-1}). The kinetic model fitted curve and detailed parameters are shown in Fig.7 and Table 3. It emerged that the HIPE30%-g-PNMG porous polymer obeyed the kinetic behavior of the PSO model, which has a higher R^2 value, and the experiment data was observed as being close to the theoretical value. It is suggested here that the limiting step was the bulk diffusion along with the spontaneous chemisorption process.

Table 3

Kinetic parameters for boron adsorption of the HIPE30%-g-PNMG.

Porous polymer	c_0 (mg/L)	PFO fitting constants			PSO fitting constants			Intraparticle diffusion	
		q_e (mmol/g)	k_1 (min^{-1})	R^2	q_e (mmol/g)	k_2 (min^{-1})	R^2	k_p (min^{-1})	R^2
HIPE30	5	0.21	0.01	0.92	0.25	0.05	0.95	0.01	0.87
%-g-	50	1.42	0.02	0.94	1.67	0.01	0.98	0.08	0.81

PNMG	100	2.66	0.01	0.97	3.47	0.03×10^{-1}	0.93	0.17	0.86

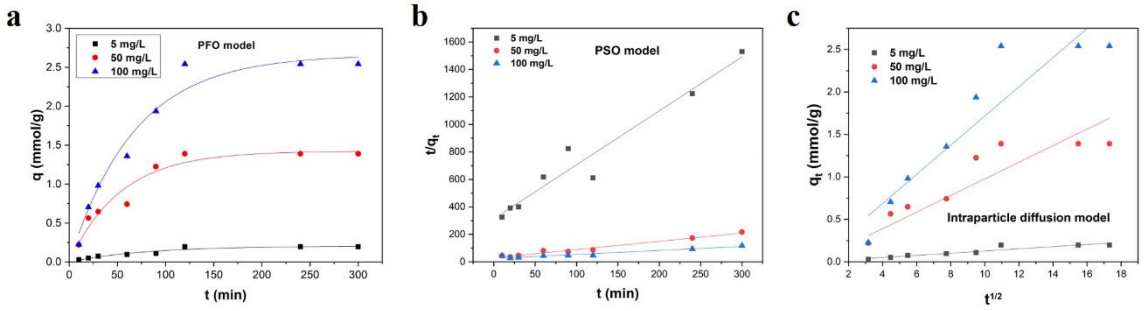

Fig. 7. Boron adsorption kinetics fitted curve of the HIPE30%-g-NMG porous polymer at different initial boron concentrations, (a) adsorption kinetics and PFO model fitted curve, (b) PSO model fitted curve, (c) Intraparticle diffusion model fitted curve

3.6. Effect of pH and regeneration test

Boric acid (H_3BO_3) is a weak acid, mainly formed from boron solution and shows a pKa value of 9.25. When the pH > 9, the $B(OH)_4^-$ occupies the dominate species while conversely, the H_3BO_3 is the dominant form presented at pH < 9. Thus, the porous polymer complexation process depended on pH sensitivity. The pH effect on boron adsorption capacity with boron solution concentration 100 mg/L is shown in Fig. 8. It revealed the obvious change in regard to the sorption data, and this was similar to our previous study [15]. In an alkaline condition, there has a mass of OH^- ion to defend the grafting vicinal hydroxyl group from the HIPE30%-g-PNMG and there was competition to form $B(OH)_4^-$. In an acidic environment, the existence of a larger number of H^+ ions promoted the process of desorption. The maximum adsorption was 2.54 mmol/g when pH=9, and it very was close to the boric acid's pKa value.

Assessing the regeneration performance is very important to establish the application and economic viability of the HIPE porous polymer. The HIPE30%-g-PNMG reuse capacity was tested through the elution process of acid and alkali treatment, and the regeneration cycle results for the evolution of the boron uptake capacity are shown in Fig. 8b. It can be seen that the HIPE30%-g-PNMG porous polymer has excellent recyclability and virtually completely maintained steady regeneration efficiency after 10 cycles. Compared with our previous analysis

of organic membrane materials, the HIPE polymer of ST and DVB matrix polymer performs outstandingly well in terms of resisting acid and alkaline conditions. We further found that the mechanical strength value of HIPE30%-g-PNMG remained at 0.73 Mpa, so it was almost unchanged after 10 cycles. Consequently, the HIPE porous polymer as an adsorbent has great potential for removing boron.

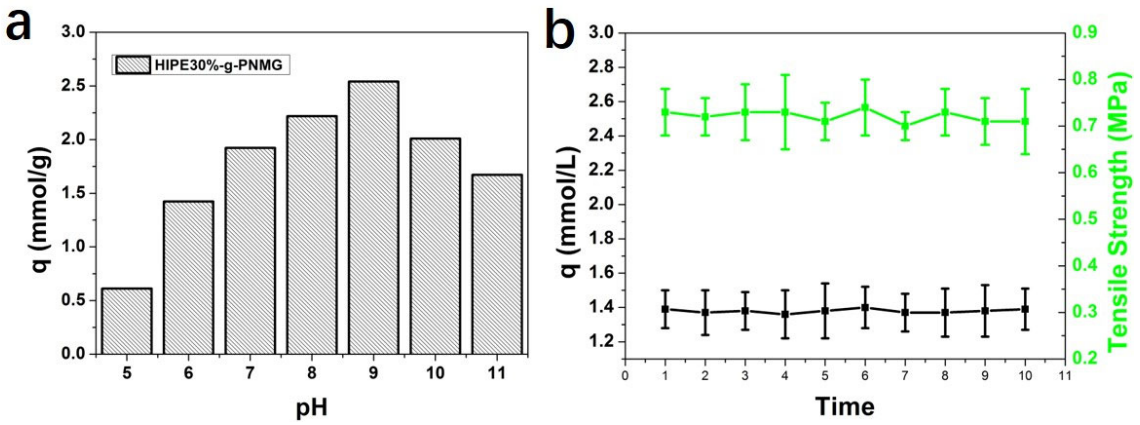

Fig. 8. (a) Influence of pH on boron adsorption (c_0 = 100 mg/L), (b) evolution of HIPE30%-g-PNMG boron uptake capacity reuse cycles in static solution (c_0 = 50 mg/L) and the changes in stress after regeneration.

4. Conclusions

HIPE porous polymer was synthesized using monomer radical polymerization and the NMG was successfully grafted onto the HIPE. This made it possible to introduce the vicinal hydroxyl group by nucleophilic substitution reaction under the catalysis of triethylamine. The obtained HIPE-g-PNMG revealed voids' sizes in the porous polymer were tunable according to different amounts of different VBC. It was verified that adding more VBC reduced the mechanical strength of HIPE-g-PNMG. The HIPE hierarchical porous structure facile made it possible to transport and adsorb the boron from the solution. Finally, the HIPE porous polymer demonstrates a great deal of potential in industrial applications.

Acknowledgements

This research was supported by the Research Project of Tianjin Education Commission (No. 2019KJ097), the National Natural Science Foundation of China (Grant No. 51671180), the National Key R&D Program of China (No.2018YFC1902401) and Tianjin Municipal Science and Technology Bureau of China (Project No. 18PTZWHZ00140).

References

[1] H.N. Liu, B.J. Qing, X.S. Ye, Q. Li, K. Lee, Z.J. Wu, Boron adsorption by composite magnetic particles, Chem. Eng. J. 151 (2009) 235–240.

[2] L.A. Melnik, Y.V. Babak, V.V. Goncharuk, I.K. Chepurnaya, Application potential of boron-selective sorbents of different nature for water conditioning in terms of the boron content, J. Water Chem. Technol. 37 (2015) 25–31.

[3] A.E. Yilmaz, R. Boncukcuoğlu, M.M. Kocakerim, B. Keskinler, The investigation of parameters affecting boron removal by electrocoagulation method, J. Hazard. Mater. 125 (2005) 160–165.

[4] J.Q. Meng, J. Yuan, Y.L. Kang, Y.F. Zhang, Q.Y. Du, Surface glycosylation of polysulfone membrane towards a novel complexing, J. Colloid Interface Sci. 368 (2012) 197–207.

[5] WHO, Guidelines for Drinking-Water Quality, fourth ed., World Health Organization, Geneva, Switzerland, 2011.

[6] S.H. Wang, Y. Zhou, C.J. Gao, Novel high boron removal polyamide reverse osmosis membranes, J. Membr. Sci. 554 (2018) 244-252.

[7] Q.Y. Ping, I.M. Abu-Reesh, Z. He, Boron removal from saline water by amicrobial desalination cell integrated with donnan dialysis, Desalination 376(2015) 55–61

[8] H.C. Tsai, S.L. Lo, Boron removal and recovery from concentrated wastewater using a microwave hydrothermal method, J. Hazard. Mater. 186 (2011)1431–1437.

[9] E. ÇermikliF. Şen, E. Altıok, J.Wolsk. P.Cyganowski, N.Kabay, M.BryjakM. Arda, M. Yüksel, Performances of novel chelating ion exchange resins for boron and arsenic removal

from saline geothermal water using adsorption-membrane filtration hybrid process, Desalination 491 (2020) 114504.

[10] M. Chen, O. Dollar, K.S. Peltier, S. Randtke, S. Waseem, E. Peltier, Boron removal by electrocoagulation: Removal mechanism, adsorption models and factors influencing removal, Water Res. 170 (2020) 115362.

[11] I. M. D. Gonzaga, A. Moratalla, K. I. B. Eguiluz, G. R. S. Banda, P. Cañizares, M. A. Rodrigo, C. Saez, Influence of the doping level of boron-doped diamond anodes on the removal of penicillin G from urine matrixes, Sci. Total Environ. 736 (2020) 139536.

[12] J. Rioyo, V. Aravinthan, J. Bundschuh, M. Lynch, 'High-pH softening pretreatment' for boron removal in inland desalination systems, Sep. Purif. Technol. 205 (2018) 308-316.

[13] B. O. Unal, D. Y. Imer, B. Keskinler, I. Koyuncu, Boron removal from geothermal water by air gap membrane distillation, Desalination 433 (2018) 141-150.

[14] W. Bouguerra, A. Mnif, B. Hamrouni, M. Dhahbi, Boron removal by adsorption onto activated alumina and by reverse osmosis, Desalination 223 (2008) 31–37.

[15] Z. Wang, P. Wang, J.J. Cao. Y.F. Zhang, B.W. Cheng, J.Q. Meng, A novel mixed matrix membrane allowing for flow-through removal of boron, Chem. Eng. J. 308 (2017) 557-567.

[16] Z. Wang, Z.Y. Wu, Y.F. Zhang, J.Q. Meng, Hyperbranched-polyol-tethered poly (amic acid) electrospun nanofiber membrane with ultrahigh adsorption capacity for boron removal, Appl. Surf. Sci. 402 (2017) 21-30.

[17] J.Q. Meng, J.J. Cao, R.S. Xu, Z. Wang, R.B. Sun, Hyperbranched grafring enabling simultaneous enhancement of the boric acid uptake and the adsorption rate of a complexing membrane, J. Mater. Chem. A 4 (2016) 11656–11665.

[18] T. Zhang, Z.G. Xu, H.G. Gui, Q.P. Guo, Emulsion-templated, microporous hydrogels for enhancing water efficiency in fighting fires, J. Mater. Chem. A 5 (2017) 10161-10164.

[19] S.Kovačič, N.Drašinac, A.Pintar, E.Žagar, Highly Porous Cationic Polyelectrolytes via Oil-

in-Water Concentrated Emulsions: Synthesis and Adsorption Kinetic Study, Langmuir 34 (2018) 10353-10362.

[20] K.K. Buchman, L. Portal, Y.J. Zhang, N. Fechler, M. Antonietti, M. S. Silverstein, Hierarchically porous carbons from an emulsion-templated, urea-based deep eutectic, J. Mater. Chem. A 5 (2017) 16376-16385.

[21] T. Zhang, M.S. Silverstein, Highly porous, emulsion-templated, zwitterionic hydrogels: amplified and accelerated uptakes with enhanced environmental sensitivity, Polym. Chem. 9 (2018) 3479-3487.

[22] L. Weinstock, R.A. Sanguramath, M.S. Silverstein, Encapsulating an organic phase change material within emulsion-templated poly(urethane urea)s, Polym. Chem. 10 (2019) 1498-1507.

[23] J. Yin, T.Q. Zhang, E. Schulman, D.X. Liu, J.Q. Meng, Hierarchical Porous Metallized Poly-melamine formaldehyde (PMF) as Low-Cost and High-Efficiency Catalyst for Cyclic Carbonate Synthesis from CO_2 and Epoxides, J. Mater. Chem. A 6 (2018) 8441-8448.

[24] J.X. Liu, J.M. Pan, Y. Ma, S.C. Liu, F.X. Qiu, Y.S. Yan, A versatile strategy to fabricate dual-imprinted porous adsorbent for efficient treatment co-contamination of λ-cyhalothrin and copper (II), Chem. Eng. J. 332 (2018) 517-527.

[25] Y.L. Zhao, Z. Zhao, J. Zhang, M.Z. Wei, X.C. Jiang, L.X. Hou, Gemini surfactant mediated HIPE template for the preparation of highly porous monolithic chitosan-g-polyacrylamide with promising adsorption performances, Eur. Polym. J. 112 (2019) 809-816.

[26] A. Barbetta, N.R. Cameron, Morphology and surface area of emulsion-derived (PolyHIPE) solid foams prepared with oil-phase soluble porogenic solvents: span 80 as surfactant, Macromolecules 37 (2004) 3188–3201,

[27] N. Kabay, M. Bryjak, S. Schlosser, M. Kitis, S. Avlonitis, Z. Matejka, I. Al-Mutaz,M. Yuksei, Adsorption-membrane filtration (AMF) hybrid process for boron removal from seawater: an overview, Desalination 223 (2008) 38–48.

[28] S. Jurjevec, E. Žagar, S. Kovačič, Functional macroporous amphoteric polyelectrolyte monoliths with tunable structures and properties through emulsion-templated synthesis, J. Colloid Interf. Sci. 575 (2020) 480-488.

[29] S. Liu, M. Jin, Y. Chen, H. Gao, X. Shi, W. Cheng, L. Ren, Y. Wang, High internal phase emulsions stabilised by supramolecular cellulose nanocrystals and their application as cell-adhesive macroporous hydrogel monoliths, J. Mater. Chem. B 5 (2017) 2671–2678

[30] J.O. Zoppe, R.A. Venditti, O.J. Rojas, Pickering emulsions stabilized by cellulose nanocrystals grafted with thermo-responsive polymer brushes, J. Colloid Interf. Sci. 369 (2012) 202–209.

[31] W.T. Chen, X.M. Yan, X.M. Wu, S.Q. Huang, Y.L. Luo, X. Gong, G.H. He, Tri-quaternized poly (ether sulfone) anion exchange membranes with improved hydroxide conductivity, J. Membr. Sci. 514 (2016) 613–621.

[32] Q.Y. Wang, H.J. Ma, J. Chen, Z.J. Du, J.G. Mi, Interfacial control of polyHIPE with nano-TiO_2 particles and polyethylenimine toward actual application in CO_2 capture, J. Environ. Chem. Eng. 3 (2017) 2807-2814.

[33] N.N. Xia, H.Y. Zhang, Z.H. Hu, G.G. Kong, F. He, A functionalized bio-based material with abundant mesopores and catechol groups for efficient removal of boron, Chemosphere 263 (2021) 128202.

[34] Y.L. Zhao, Z. Zhao, J. Zhang, M.Z. Wei, X.C. Jiang, L.X. Hou, Gemini surfactant mediated HIPE template for the preparation of highly porous monolithic chitosan-g-polyacrylamide with promising adsorption performances, Eur. Polym. J. 112 (2019) 809-816.